arXiv:physics/0201034v1 [physics.atom-ph] 16 Jan 2002

An Intense Source of Cold Rb Atoms from a Pure 2D-MOT

J. Schoser, A. Batär, R. Löw, V. Schweikhard, A. Grabowski, Yu.B. Ovchinnikov, and T. Pfau
5.Physikalisches Institut, Universität Stuttgart, Pfaffenwaldring 57, 70550 Stuttgart, Germany
(Dated: February 2, 2008)

We present a 2D-MOT setup for the production of a continuous collimated beam of cold ^{87}Rb atoms out of a vapor cell. The underlying physics is purely two-dimensional cooling and trapping, which allows for a high flux of up to $6 \cdot 10^{10}$ atoms/s and a small divergence of the resulting beam. We analyze the velocity distribution of the 2D-MOT. The longitudinal velocity distribution of the atomic beam shows a broad feature(FWHM$\simeq$75 m/s), centered around 50 m/s. The dependence of the flux on laser intensity, geometry of the trapping volume and on pressure in the vapor cell was investigated in detail. The influence of the geometry of the 2D-MOT on the mean velocity of the cold beam has been studied. We present a simple model for the velocity distribution of the flux based on rate equations describing the general dependencies.

Cold atomic beams are needed for many applications in atom optics [1, 2] or in the field of atomic clocks based on atomic fountains. Especially the process of evaporative cooling [3] demands a high atom number as a starting point for reaching quantum degeneracy. This requires an intense source which can efficiently load a magneto-optical trap (MOT) fast.

For this purpose sources with a small divergence of the atomic beam are favorable. The longitudinal velocities in the beam should be within the capture range of the 3D-MOT. As long as the cross section of the beam is smaller than the spatial capture range of the MOT the figure of merit for optimized loading into a MOT is the total integrated flux up to its capture velocity.

Besides background gas loading and pulsed loading mechanisms like chirped slowers or double-MOT systems many experiments use Zeeman slowers as a continuous source [4]. A Zeeman-slower decelerates an intense thermal atomic beam along the propagation axis of the beam by radiation pressure, while the spontaneous emission processes give rise to a transverse heating of the atoms. This emerges in a strongly diverging beam with a flux of up to 10^{11} atoms/s. In some cases the slowing light on axis or the magnetic fields involved disturb the consecutive MOT.

Lu et al. [5] have realized a low velocity intense source (LVIS) of atoms by creation of a dark channel in one of the six MOT-laser-beams. Due to the imbalance in the radiation pressure along one axis a continuous beam of cold atoms is coupled out of a trapped cloud. This source provides a small thermal background and a narrow velocity profile at velocities below 20 m/s. However it does not reach the high flux of a Zeeman slower.

A new approach is 2-dimensional magneto-optical cooling and trapping. This technique has first been used to extract very slow atoms out of a cooled atomic beam by Riis et al. [6] and was later refined to produce a beam of slow atoms with velocities from 2 to 10 m/s [7, 8]. An alternative is to collimate and compress a slow atomic beam like realized by [9, 10]. Finally it has been demonstrated that an atomic funnel, applied in different configurations, produces a beam of cold atoms out of a vapor cell [11, 12, 13]. Dieckmann et al. have realized a 2D$^+$-MOT which produces a total flux of $9 \cdot 10^9$ Rb^{87}-atoms/s. The plus-sign stands for a pushing laser beam on axis copropagating with the atomic beam. This setup uses small cooling laser powers and retroreflection of the laser beams. The vapor pressure reaches up to saturated vapor pressure ($\simeq 10^{-7}$ mbar) at room temperature.

Pure 2D cooling does not require light on the axis of the atomic beam compared to a Zeeman slower, an LVIS or a 2D$^+$-MOT. Hence there is less disturbance of the consecutive 3D-MOT setup. Radial cooling collimates the outgoing beam while the allowed cooling time, which depends on the geometry of the cooling region, influences the possible longitudinal velocities of atoms in the beam. The resulting flux is comparable to the one of a Zeeman slower. Moreover it offers a small beam-divergence. In our system we could achieve a flux of $6{\cdot}10^{10}$ atoms/s with a beam-divergence of 32 mrad. The figure of merit characterizing the performance of our system is the integrated brightness which is about $2 \cdot 10^{12}$ atoms/(s·srad). On the other hand one needs to accept a rather high mean velocity of the cold beam and a relatively broad velocity distribution depending on the chosen geometry. The mean velocity of the atoms in our apparatus is $\simeq$50 m/s. We plan to capture most of the atoms up to a capture velocity of 60 m/s by a large volume, elongated 3D-MOT in a UHV-chamber which the atomic beam enters at a small angle with respect to the long axes of the elongated MOT.

This paper is organized as follows: in section I we explain the basic principle of a two-dimensional MOT. We discuss the influence of geometry, laser power and pressure in the vapor cell on the atomic beam. Based on rate equations we derive a model for the longitudinal velocity distribution. Section II gives a detailed description of the setup and the measurement techniques used for the characterization. We present the results and discuss the applicability of our model in part III. We summarize and give an outlook on future steps in our experiment in section IV.

I. PRINCIPLE OF OPERATION AND THEORETICAL MODEL

The basic geometry of the experimental setup (see Fig. 1) is given by a vapor cell separated from a UHV-chamber by a differential pumping tube which is also the aperture for the output beam of cold atoms. A two-dimensional magnetic quadrupole field is produced by four coils with rectangular shape. The axis of both, the cell and the tube, coincide with the line of zero magnetic field. Four perpendicularly counterpropagating laser beams with orthogonal circular polarisations in the usual MOT-configuration enclose a cooling volume along the axis of zero magnetic field (z-axis). The center of the MOT laser beams is positioned about 4 cm in front of the differential pumping tube. The cooling volume extends to the entrance of the tube. Atoms in the vapor cell which enter the cooling volume are slowed down in the two radial dimensions and are compressed to the z-axis. The atoms' velocity in the longitudinal direction is not cooled. Hence the atoms experience a skew trajectory into the center of the 2D-MOT, according to the equation of motion of a damped harmonic oscillator, while propagating along the axis. This produces a thin, dense, well collimated atomic beam in two directions, namely in the positive and negative z-direction. We constrict ourselves to one beam travelling in the positive z-direction, where it passes through the differential pumping tube. The other beam is lost after it hit the back wall of the glass cell.

The atoms in the vapor cell have to fulfill three criteria simultaneously in order to contribute to the flux of laser-cooled slow atoms at the exit of the differential pumping tube:

a) The initial radial velocity component needs to be smaller than the transverse capture velocity of the 2D-MOT.

b) The interaction time of the atoms with the light field needs to be long enough so that the trajectory of the atom hits the entrance of the differential pumping tube (the radial velocity is sufficiently cooled) such that its divergence is small enough to make it to the exit of the tube.

c) The mean free path in the vapor cell should be larger or comparable to the length of the 2D-MOT, so that the cooling of the atoms has not suffered from collisions.

At first we consider the collision-less regime. Here the density is low enough that the mean free path in the vapor cell is larger than the dimensions of the cell. In this case we can assume that the thermal atoms start on the walls and no collisions take place in the volume. The geometry of the tube and the glass cell is designed in such a way that the opening angle of the differential pumping tube does not accept atoms starting on the side walls without being transversely cooled. In this configuration thermal atoms are only transmitted if they start on that part of the back wall of the glass cell which lies within the acceptance angle of the differential pumping tube. This choice limits the thermal background.

For an understanding of the total flux and its dependence on the geometry, the longitudinal velocity profile of the atomic beam needs to be investigated. This information is given by the range of accepted velocity classes and its dependence on external parameters. The concept of a capture velocity, well-known from 3D-magneto-optical-traps, must be modified to embrace the 2D-MOT-configuration. Since the cooling is restricted to transverse velocities, we define a radial capture velocity. In spherical 3D-MOTs the capture velocity has a constant value depending only on detuning, laser beam size and intensity and on the magnetic field gradient. However, in a 2D-MOT a finite cooling time is necessary to collimate the atoms onto the beam axis. Atoms which travel too fast along the z-direction can not be sufficiently cooled and are filtered out by the aperture. A main parameter is therefore the cooling time $\tau = z/v_z$ which is given by the longitudinal velocity v_z and the distance z from the tube at which the atom enters the cooling volume of the 2D-MOT. Thus the effective transverse capture velocity becomes a function of z and v_z. For small v_z the radial cooling time dominates and the capture velocity should be simply a constant v_{c0} determined by the parameters of the cooling laser beams and the magnetic field gradient. For larger v_z the capture velocity should fall off as $1/v_z$. The velocity range between these two asymptotes depends additionally on the position z where atoms enter the cooling volume. With increasing cooling length one should expect more atoms with high axial velocities to be transversely cooled and transmitted through the tube.

The cooling time τ determines the final transverse velocity: $v_{r,i} - v_{r,f} = \frac{1}{m}\int_0^\tau F_{sp}(x(t), v(t))dt$. Here F_{sp} is the spontaneous scattering force, $v_{r,i}$ the initial, $v_{r,f}$ the final radial velocity and m the mass of a Rb-atom. By that the divergence of the atomic beam (if it is not limited by the acceptance angle of the tube) is shaped depending on the mean length of the cooling volume. Radial cooling within a finite cooling time increases the portion of atoms with small v_z in the beam. *This is the reason why the velocity distribution of the atomic beam is non-thermal and is shifted to much lower values than a thermal distribution* at room temperature ($\langle v \rangle \simeq 275$ m/s) although there is no longitudinal cooling. A typical time scale for the cooling time is 1-2 ms. As will be described in part II, a usual length of the cooling volume in our setup is about 60 mm. This gives a rough estimation for the mean velocity in the atomic beam between 30 and 60 m/s.

The influence of the MOT-laser intensity is reflected in the efficiency of the transverse cooling. The capture velocity should increase with intensity and saturate at some value when the saturation parameter dominates the spontaneous force.

The vertical beam size, in combination with detuning

and magnetic field gradient, determines the radial capture velocity v_{c0}. An increase of the length of the 2D-MOT increases the upper limit of the longitudinal velocities which are trappable. Additionally, the size controls the mean longitudinal velocity in the beam of cold atoms which increases with increasing MOT-length. Hence the total flux should grow with the length of the 2D-MOT. In the limit of an infinitely long 2D-MOT the longitudinal velocity distribution of the atom beam becomes equal to a thermal distribution.
Without collisions the number of trappable atoms and thereby the flux increases with a higher pressure in the vapor cell.
Let us now discuss the effect of collisions. At higher pressures their evolution creates a thermalization of the atoms in the volume of the vapor cell. Thereby atoms can now start not only from the walls but also from within the vapor cell. This increases the background of thermal atoms in the atomic beam. Moreover background gas collisions in the vapor cell and light assisted collisions of excited atoms in the beam with the background gas are mechanisms that limit the flux when the MOT-length increases. The mean number of collisions is given by the product of an ensemble averaged collision rate $\Gamma = n\,\sigma\,\langle v\rangle$ and the mean time $\tau = \langle z\rangle / v_z$ which the atom spends in the cooling volume. n is the density in the vapor cell, σ the collision cross section and $\langle v\rangle$ the mean thermal velocity in the vapor cell. The longer the MOT is, the longer becomes the time of propagation which the atoms spend in the vapor cell. Therefore the higher is the probability for losses due to collisions such that a further increase of MOT-length does not produce a higher flux. In this simple picture the flux is supposed to saturate as a function of MOT-length. The mean velocity should increase since atoms with small v_z are more vulnerable by collisions.
For a given MOT geometry an increasing pressure will decrease the effective length of the cooling volume. Therefore one should expect an optimum pressure for a given geometry of the 2D-MOT, namely when the mean free path in the vapor cell becomes comparable with the length of the cooling volume. In addition higher densities in the vapor cell lead to a higher absorption of the light beams and decrease the cooling efficiency.

For a theoretical description of the flux of cold atoms from a 2D-MOT source we resort to a simple rate model which was introduced in [14] for vapor-cell MOTs and later expanded for atomic beam sources in [12]. Based on that model for the total flux we derive a model for the longitudinal velocity distribution of the atom flux.
We define a function $\hat{\Phi}$ which describes the integrated flux per velocity interval $[v_z, v_z + dv_z]$:

$$\hat{\Phi}(n, v_z) = \frac{\int_0^L R(n, v_z, z) \cdot \exp\left(-\Gamma_{coll}(n)\frac{z}{v_z}\right) dz}{1 + \frac{\Gamma_{trap}(n)}{\Gamma_{out}}} \quad (1)$$

Here Γ_{trap} is the loss rate out of the trapped cloud due to background gas collisions, Γ_{out} determines the outcoupling rate from the captured vapor in the 2D-MOT-trapping region into the atomic beam. L is the total length of the cooling volume and n is the density of Rb-atoms in the vapor cell. R is the loading rate of ^{87}Rb atoms into the 2D-MOT. The effect of light assisted collisions between the background gas and the cold atoms in the atomic beam on the way to the tube (described by the collision rate Γ_{coll}) is implemented by an exponential loss term. In our setup the cooling region extends directly to the differential pumping tube. z/v_z is the time of flight for the atoms through the MOT-volume.
The total flux, which gives the number of atoms per time interval integrated over the output area of the source, is given by the integral of $\hat{\Phi}$ over all longitudinal velocities: $\Phi = \int_0^\infty \hat{\Phi}(n, v_z)\, dv_z$. Only positive values for v_z are taken into account.
In order to derive the loading rate for a 2D-MOT, one needs to consider the flux of atoms through the surface of the cooling volume. Since we are interested in the loading flux through the side walls, we need to consider only radial velocities, weighted with that part of the Boltzmann distribution which is trappable according to the discussion above. The loading rate is proportional to the density in the vapor cell and to the surface area of the cooling volume. For simplicity we take a cylindrical cooling volume. We define a loading rate per velocity interval $[v_z, v_z + dv_z]$:

$$R(n, v_z, z) = n\, d\, \frac{16\sqrt{\pi}}{u^3} \exp\left(\frac{-v_z^2}{u^2}\right) \cdot \int_0^{v_c(v_z,z)} v_r^2 \exp\left(\frac{-v_r^2}{u^2}\right) dv_r \quad (2)$$

Where d is the diameter of the cooling volume, $u = \sqrt{\frac{2k_B T}{m}}$ is the most probable velocity of the Maxwell-Boltzmann-distribution with k_B denoting the Boltzmann constant and T the temperature of the vapor, $v_r = \sqrt{v_x^2 + v_y^2}$ is the radial velocity. The integral's upper limit v_c is the capture velocity which is generally a function of the longitudinal velocity v_z and of the atom's distance z from the aperture.
To satisfy the two asymptotic behaviors at low v_z ($v_c \to v_{c0} = const$) and at high v_z ($v_c \propto 1/v_z$) we model v_c as:

$$v_c(v_z, z) = \frac{v_{c0}}{1 + \frac{v_z}{v_{cr}}} \quad (3)$$

v_{c0} is the radial capture velocity which lies usually in the range of 30 m/s. v_{cr} is the so called critical velocity above which the cooling time is limited by the longitudinal motion and the capture velocity falls off as $1/v_z$. The capture velocity is nearly equal to v_{c0} below v_{cr}. We choose v_{cr} via the equality of the mean longitudinal flight time $L/(2\,v_{cr})$ and the radial cooling time which we approximate by d/v_{c0}. In this approximation the explicit z-dependence drops out of v_c. This results in: $v_{cr} = L\,v_{c0}/(2\,d)$.

This gives for the flux per velocity interval:

$$\hat{\Phi}(n, v_z) = \frac{nd}{1+\frac{\Gamma_{trap}(n)}{\Gamma_{out}}} \frac{16\sqrt{\pi}}{u^3} \frac{v_z}{\Gamma_{coll}} \exp\left(\frac{-v_z^2}{u^2}\right) \left(1 - \exp\left(-\Gamma_{coll}\frac{L}{v_z}\right)\right) \int_0^{v_c} v_r^2 \exp\left(\frac{-v_r^2}{u^2}\right) \quad (4)$$

At residual vapor pressures of a few 10^{-7} mbar the typical lifetime of a MOT loaded from atomic beams is about 100 ms. From that we conclude a collision rate Γ_{trap} on the order of $10\,\mathrm{s}^{-1}$ for this vapor pressure. As will be discussed in part III the typical cooling time is in the range of ms therefore the order of magnitude for Γ_{out} is $10^3\,\mathrm{s}^{-1}$. The collision rate for light assisted collisions is given by: $\Gamma_{coll} = n\,\langle v\rangle\sigma$. $\langle v\rangle$ is the mean velocity in the vapor, σ is the effective collision cross section for light assisted collisions between background gas atoms and atoms in the cold beam. Following [12, 15] we assume that this process can be described by resonant dipole-dipole interaction and follows a C_3/R^3 potential. R is the inter-atomic distance.

When fitting the experimental results with this theoretical model we obtain $\Gamma_{trap}/\Gamma_{out} = 0.012$ at a pressure of 10^{-7} mbar. This agrees well with the observed lifetimes. For the effective collision cross section we get: $\sigma_{eff} \approx 1.8 \cdot 10^{-12}\,\mathrm{cm}^2$. This value matches within a factor of two with the measurement of Dieckmann et al. [12].

When comparing the theoretical results with the experiment, equation (4) needs to be multiplied by an overall efficiency factor. The fit to our measured data yields an efficiency factor of $5 \cdot 10^{-3}$. This takes into account the different intensities, the Gaussian beam profiles and the absorption in the Rb-vapor. Equation (4) describes the longitudinal velocity distribution in the cold atomic beam. A comparison of this model with the measured results will be given in part III.

Let us summarize the expected general behavior:

1) An increasing MOT-length should lead to:

a) *a higher flux.* Faster atoms can be captured with an increasing L. Due to collisions the expression of $\hat{\Phi}(n, v_z)$ becomes independent of L for large values of L. The flux shows a saturation for lengths above $L > \frac{\langle v_z\rangle}{\Gamma_{coll}(n)}$.

b) *an increasing mean velocity in the atomic beam.* Above an optimum MOT-length every increase in length will only add faster atoms to the beam, thus increasing the value for the mean velocity.

2) An increasing density of Rb-atoms in the vapor cell should lead to:

a) *a linear increase of the total flux at low pressures.* The loading rate is proportional to $\frac{n}{1+\Gamma_{trap}(n)/\Gamma_{out}}$ which is linear in the density for low pressures. At higher pressures the term $1/\Gamma_{coll}(n)$, which is inversely proportional to n, dominates. For a given length of the MOT-beams there exists an optimum pressure above which the flux decreases with increasing pressure.

b) *an increasing mean velocity.* The necessary momentum transfer to be pushed out of the beam is smaller for the slow atoms, leaving a higher fraction of hotter atoms in the beam.

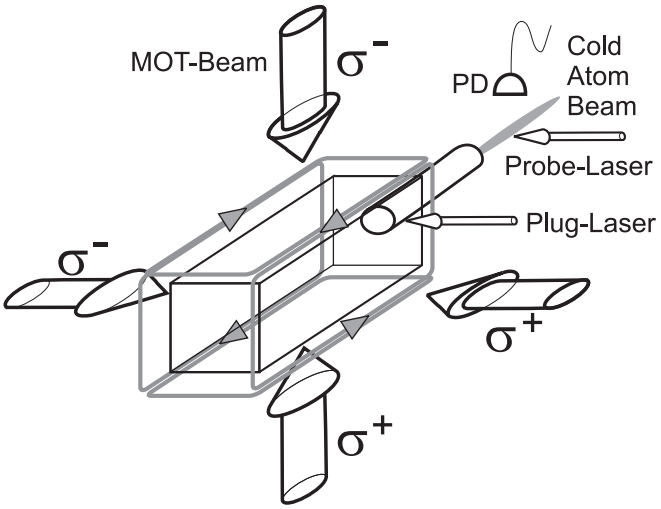

FIG. 1: Schematic view of the setup. Rectangular coils produce a 2-dimensional magnetic quadrupole field. The line of zero magnetic field coincides with the long axis of the glass cell. Four perpendicular laser beams with circular polarizations in the usual MOT configuration cool the atoms in two dimensions. The atomic beam travels horizontally through a differential pumping tube. Analysis of the beam is done by a time-of-flight-method. A plug beam shuts off the atomic beam and a probe-laser is shone in perpendicularly to the beam. The fluorescence is detected by a calibrated photodetector.

II. EXPERIMENTAL SETUP AND DIAGNOSTICS

As discussed in the previous section the main parameters leading to a high flux are the length of the cooling volume and a high vapor pressure. In our apparatus we tried to optimize these parameters.

Our setup consists of a 2-chamber vacuum-system separated by a differential pumping tube. The tube is conically shaped, 133 mm long and has a diameter of 6 mm which widens at the UHV-end up to 9.6 mm. It maintains a pressure drop of three orders of magnitude between a vapor pressure cell and two UHV-six-way-crosses used as analyzing chambers. Compared to other setups we use a rather large aperture for the differential pumping tube. The vapor cell is a glass cuvette (135mm x 35mm x 35mm) whose long axis (z-axis) is horizontally aligned. The geometry is chosen in such a way that the opening angle of the tube does not permit atoms starting on the side walls to be transmitted without transverse cooling. The purpose of this tube is mainly to separate the cold atomic beam from the thermal atoms. Electric heating rods around the glass cell provide homogeneous and stable heating thus allowing to work

at relatively high vapor pressures between 10^{-7} and $3 \cdot 10^{-6}$ mbar. Four rectangularly shaped, elongated magnetic coils are placed around the vapor-cell producing a two-dimensional quadrupole field. The zero magnetic field line is along the axis of the glass cell. We work with a field gradient of 17 G/cm. A schematic view of the setup is depicted in Fig. 1.

Cooling laser light is provided by a Ti:Sapphire-laser. The laser is red-detuned by $1.9\,\Gamma$ from the $5S_{1/2}$,F=2 $\longrightarrow$ $5P_{3/2}$,F=3 transition. To repump atoms back into the cycling transition an external cavity diode laser is employed which is stabilized to the $5S_{1/2}$,F=1 $\longrightarrow$ $5P_{3/2}$,F=2 transition. For the analysis of the atomic beam another diode-laser is used. This probe-laser is locked on resonance to the $5S_{1/2}$,F=2 $\longrightarrow$ $5P_{3/2}$,F=3 transition.

The light of the cooling laser is split into four separate beams which are expanded in spherical and cylindrical telescopes placed in sequence up to a beamsize of roughly 95x15 mm (horizontal waist radius $w_z \approx 25$ mm, vertical waist radius $w_\rho \approx 6$ mm). Two pairs of horizontally and vertically counterpropagating beams are overlapped in the center of the glass cell. The repumping light is overlapped with two horizontal beams. In order to work at high vapor pressures it is necessary to use four different laser beams. Retroreflection of the light beams would lead to a strong imbalance in the light pressure due to the high absorption in the vapor.

The cooling volume extends to the front of the differential pumping tube. The center of the 2D-MOT is about 40 mm in front of the entrance edge of the tube. There is no dark distance which the atoms travel at background pressure without being transversely cooled. This upholds the good collimation of the beam until it leaves the vapor cell.

Diagnostics

The measurement of the Rb-pressure in the cell is accomplished by absorption measurement. The frequency of a small laser beam whose intensity is below saturation is swept across resonance. The measurement is calibrated by the absorption of Rb-vapor at room temperature whose vapor pressure is 10^{-7} mbar [17].

Information about the transverse capture velocity of the 2D-MOT can be obtained by Doppler-spectroscopy perpendicular to the atomic beam. For that purpose a probe-laser beam with a diameter of 1 mm is aligned through the atomic beam orthogonally to its axis onto a photodiode. When sweeping its frequency across resonance the Doppler-profile reveals a Gaussian-shape due to the thermal velocity distribution of the atoms with two dips symmetrically centered around the maximum. Atoms of the velocity classes corresponding to the dips have been cooled and therefore the height of the central part corresponding to the cold atoms increases. Division by the fitted Gaussian-profile shows this structure clearly (Fig. 3). Half of the width between the minima corresponds to the capture velocity.

The transverse beam profile is investigated in the UHV-part of the setup. A probe-beam with a diameter of 1 mm is directed orthogonally on the atomic beam. Perpendicular to it a CCD-camera images the fluorescence signal. From the increasing width (FWHM) of the signal when moving the probe beam along the z-axis the divergence of the atomic beam is quantified.

The analysis of the longitudinal velocity distribution of the atomic beam is done by a time of flight (TOF) method. A fraction of the MOT-laser intensity is split apart and shone into the vapor cell directly in front of the tube perpendicular to the atomic beam axis. This beam has a diameter of ≈ 8 mm, and its intensity was held at 150 mW throughout all measurements. It deflects all atoms with a longitudinal velocity lower than 130 m/s and hence plugs the atomic beam for all smaller velocities. After a flight-distance of 145 mm a light-sheet of 1 mm width from a probe laser is irradiated on the atomic beam in the UHV-chamber orthogonal to the atom beam. A fraction of the repumping light is overlapped with the probe-laser. A calibrated photodiode detects the fluorescence of the atoms. After plugging the atomic beam the fluorescence signal fades out. From this signal information about the velocity distribution of the atomic flux can be derived according to:

$$\Phi(v_z) = \frac{\eta}{d_{probe}} \frac{l}{v_z} \frac{dS}{dt} \tag{5}$$

Where S is the signal from the photodiode, d_{probe} the width of the probe-beam light-sheet, l the distance between plug-beam and probe-beam and η contains calibration parameters of the detection system.

III. EXPERIMENTAL RESULTS

At first we give information about the characteristics of the 2D-MOT: its loading time and its capture velocity. This is followed by a discussion of the properties of the atomic beam. The influence of laser power, length of the cooling volume and of the pressure in the vapor cell is studied.

The two-dimensional laser-cooling produces a about 2 mm thin, 90 mm long, line of high intensity of fluorescence light in the glass cell along the axis of zero magnetic field which is clearly visible at low vapor pressures. A picture of the fluorescence light in the 2D-MOT is shown in Fig. 2.

A measurement of the radial capture velocity in the above described way yields the maximum transverse capture velocity v_{c0} in equation (3). The capture velocity depends merely on the intensity of the laser beams, the detuning and on the magnetic field gradient. Figure 3 displays the dependence of v_{c0} on the laser intensity. The inset shows the Doppler-spectroscopy signal from which the capture velocity is inferred. In the intensity

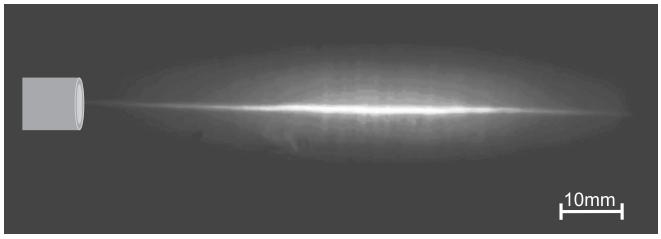

FIG. 2: Picture of the fluorescence in the 2D-MOT with a flux of $3.5 \cdot 10^{10}$ atoms/s. The vapor pressure in the glass cell is about $7 \cdot 10^{-7}$ mbar. A beam of approximately 90 mm length and a thickness of 2 mm develops. The cooling region extends to the differential pumping tube which is sketched on the left.

range which we apply, it extends from 28 m/s to 38 m/s. For high laser powers above 160 mW per beam (which corresponds to an intensity of $\simeq$17 mw/cm^2) it saturates at a value of 38 m/s. This value matches well with an estimation when equating the frequency shift due to the Zeeman effect with the detuning of the laser, which gives the linear capture range - in our case 35 m/s.

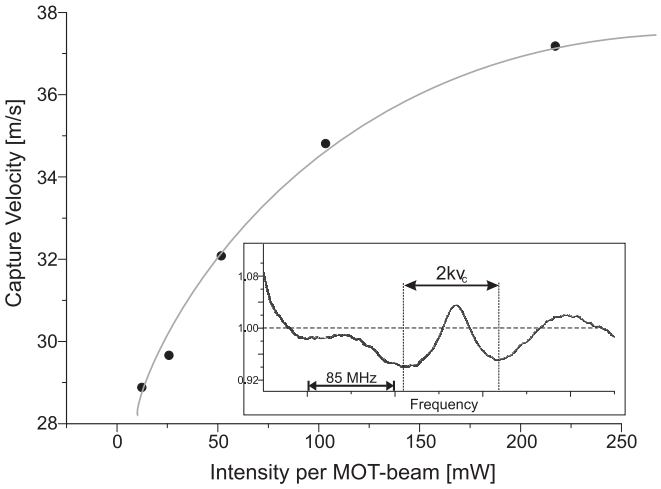

FIG. 3: Transverse capture velocity of the 2D-MOT. The inset shows the normalized Doppler-spectroscopy signal, i.e. the measured signal divided by a fitted Gaussian distribution. The width between the two minima corresponds to twice the capture velocity. The main graph shows the dependence of the capture velocity on the intensity in the cooling laser beams. The line serves merely to guide the eye. The capture velocity saturates at high intensities at a value of 38 m/s.

For measuring the loading time of the 2D-MOT we directed a 1 mm thick probe laser beam through the center of the atomic beam onto a photodiode. When switching on the 2D-MOT cooling light the absorption decreased abruptly because the F=2 $\longrightarrow$F=3-transition is driven by the MOT laser. The absorption increases again and reaches a steady state when the atoms are transversely cooled and closer in resonance with the probe laser than with the MOT light. The $1/e$-time of this increase is about 2 ms. This gives the characteristic time scale for the cooling process. From that we can estimate the value for the outcoupling rate Γ_{out} in equation (4) to be on the order of $10^3\,\mathrm{s}^{-1}$.
The emerging atomic beam is well collimated. From our transverse beam profile measurement we deduce a beam-divergence of 32 mrad. This is about a factor of 2 less than the geometrically allowed divergence by the differential pumping tube of 59 mrad. This means that the beam of cold atoms is not hindered by the aperture. It is possible to further suppress the thermal background by diminishing the aperture of the differential pumping tube without decreasing the flux of cold atoms in future experiments.

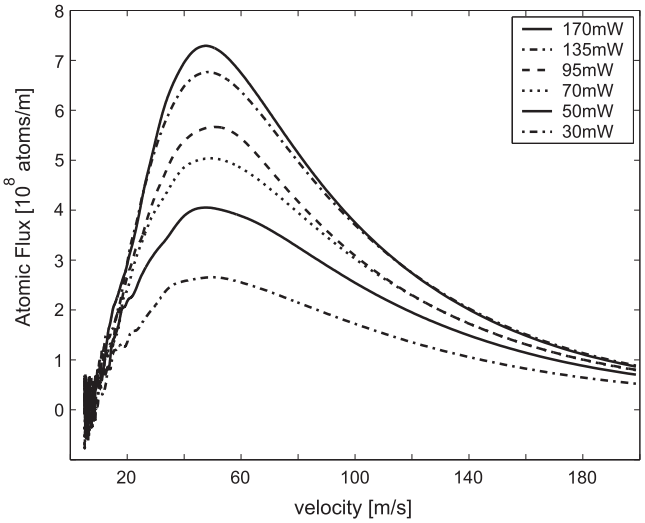

FIG. 4: Distribution of the atomic flux versus the longitudinal velocity. The laser power in the cooling beams was varied from 30 mW to 170 mW. The pressure for this measurement is $1.6\,10^{-6}$ mbar, the length is 92 mm. A small shift of the mean velocity to higher values with increasing laser power is visible. The velocity distribution is centered around 50 m/s and has a width of about 75 m/s.

The time-of-flight measurements give information about the distribution of the atomic flux versus velocity. A typical set of velocity distributions is depicted in Fig. 4. The varied parameter for the single curves is the power in the laser beams. We observe a relatively broad feature with a peak velocity of around 50 m/s and a width of roughly 75 m/s. An increase of the peak velocity with increasing laser power is visible. The transverse cooling works more efficiently with increasing laser intensity. Therefore atoms with a higher velocity in the z-direction contribute to the beam. The integral of the flux-distribution gives the total flux of atoms per unit time. This is displayed in Fig. 5. The total flux saturates for laser powers above 160 mW per laser beam. We observe a maximum flux of $6{\cdot}10^{10}$ atoms/s at a laser

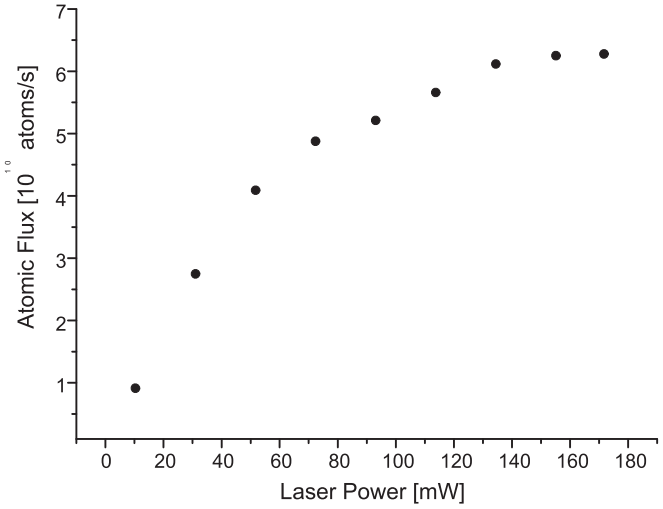

FIG. 5: Dependence of the total atomic flux on the cooling laser power per beam. The total flux in atoms/s is given by the area under the curves in graph 4. It ranges from $1 \cdot 10^{10}$ to $6 \cdot 10^{10}$ atoms/s. The total flux depends strongly on laser power and saturates at values of 160 mW per laser beam.

power of 160 mW per laser beam and at a vapor pressure of $1.8 \cdot 10^{-6}$ mbar.

In addition to the field gradient and the detuning, the size of the MOT-beams determines the capture range of the MOT. As discussed in part I the length of the cylindrical MOT-beams strongly influences the flux of cold atoms. Fig. 6 shows the distribution of the atomic flux versus velocity when the length of the beams is varied. The upper part shows the result of our theoretical model. The lower part displays the TOF-results. This measurement was done by successively blocking a part of all four cylindrical MOT-beams starting on the back side of the glass cell while simultaneously increasing the laser power per beam. Thus the total power shining on the atoms is kept constant and it is ensured that we see a pure influence of the MOT-length. With increasing length the flux grows and the maximum velocity shifts to higher values. Fig. 7 shows the total flux as a function of the MOT length. The total flux is expected to saturate for a cooling volume above an optimum length which is given by the mean velocity and the collision rate $\Gamma_{coll}(n)$ as discussed in part I. However, for the pressure range of this measurement no saturation of the flux is visible even at the maximum MOT-length of 92 mm. The discussion of the geometry dependence of the total flux clearly reveals the advantage of utilizing the whole laser power across a long cooling volume compared to increasing the laser intensity in a usually sized MOT.
The longer the MOT the longer is the interaction region for the atoms to be transversely cooled. Therefore also higher velocity classes can be gathered into the beam. This explains that the maximum velocity is shifted towards higher values with increasing MOT-length.

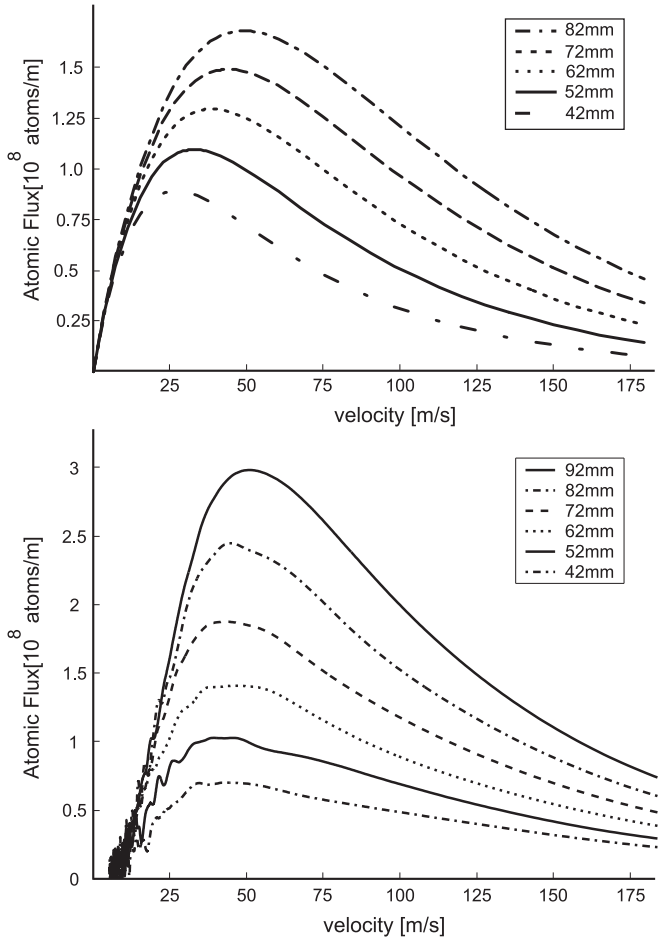

FIG. 6: Dependence of the atomic flux on the length of the MOT-beams. The upper graph shows the prediction by our model. The experimental result is plotted in the lower graph. The power per laser beam is held constant at 21 mW and the Rb-pressure is $1.6 \cdot 10^{-6}$ mbar. The peak of the velocity distribution is shifted to higher values for a longer cooling volume. The atomic flux increases with the length of the cooling volume. In this measurement an increasing part of the MOT-beams is blocked while the laser power is adjusted so that the total laser power incident on the atoms stays constant.

With an increasing length the mean velocity becomes larger. For an infinitely long 2D-MOT and low vapor pressures the velocity distribution should approach a thermal distribution. In applications like loading a 3D-MOT, the choice of the 2D-MOT length is limited by the 3D-MOT's maximum capture velocity.
Our model is in good agreement with the measurements and predicts the essential features that we observe. Only the width of the velocity distribution is not accurately predicted.

The variation of the Rb-vapor pressure is done by changing the temperature of the glass cell in a controlled way. It is possible to raise the vapor pressure from $1 \cdot 10^{-7}$ mbar to $3 \cdot 10^{-6}$ mbar. Fig. 8 demonstrates the dependence of the velocity distribution on the

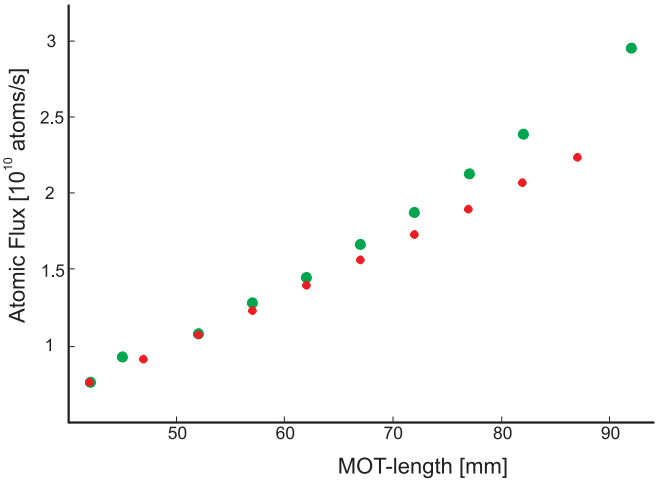

FIG. 7: Dependence of the total flux on the length of the cooling volume. The experimental parameters are the same as in Fig. 6. The dark spots show the theoretical the bright circles the experimental data.

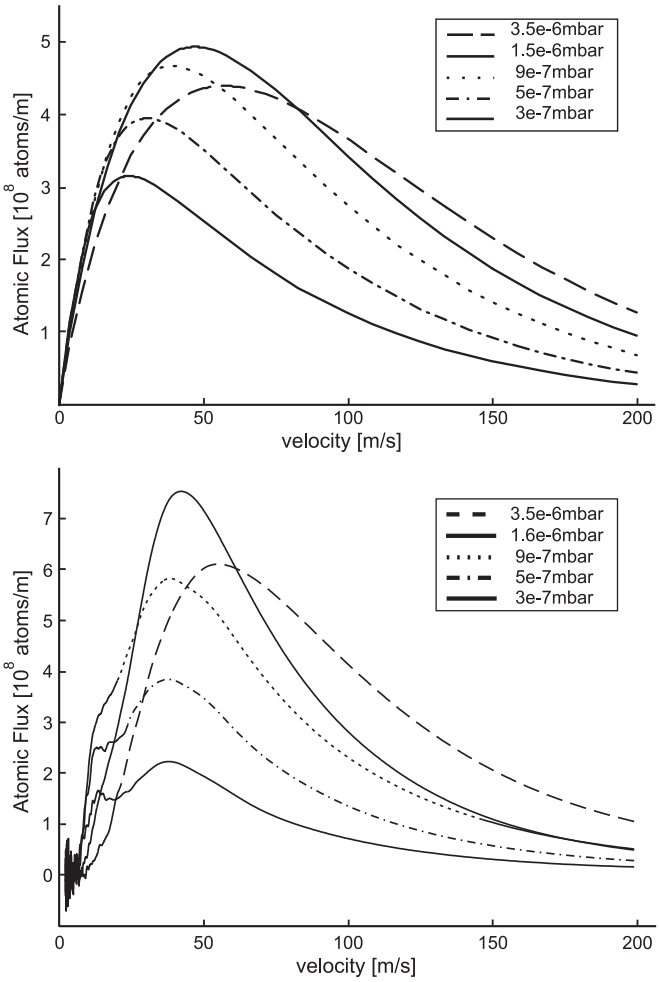

FIG. 8: Distribution of the atomic flux versus the longitudinal velocity. The pressure in the vapor cell was varied from 10^{-7} mbar to $3.5 \cdot 10^{-6}$ mbar. The upper graph shows the results of our model. The experimental results are plotted in the lower graph. The model describes an increase in the peak velocity with increasing pressure and also a growing flux with higher pressures which is in accordance with the experimental results. Above an optimum pressure the flux decreases again. This is also visible in the dashed line both in the model and in the measurement.

vapor pressure. The upper part shows the behavior as described by our theoretical model, the lower graph displays the TOF-measurements. The flux increases with increasing pressure, reaches a maximum at $1.5{\cdot}10^{-6}$ mbar and decreases again for higher pressures. In the high pressure regime the mean free path of Rb-atoms in the vapor cell is on the order of a few cm and is comparable to the dimensions of the atomic beam in the 2D-MOT. This means that collisions start to limit the atomic flux as is discussed in part I. Above the optimum pressure value the total flux decreases again. The optimum pressure depends on the length of the 2D-MOT. The longer the 2D-MOT the smaller is the value for the optimum pressure. Our value for the optimum pressure agrees well with the prediction of Vredenbregt et al [16]. The maximum velocity of the distribution shifts towards higher values with increasing pressures. This is revealed in the experiment and also in the theoretical curves. Atoms with a small longitudinal velocity are more vulnerable by collisions because a small transverse momentum transfer already produces a large enough divergence so that the atoms collide with the tube. A higher pressure leads to a larger mean velocity in the atomic beam.

The total flux as a function of vapor pressure is shown in Fig. 9. The linear increase of the flux at low pressures and the existence of an optimum pressure is well described by our model.

In addition to the Doppler-cooling laser light we shone in a laser beam of the same detuning on the axis copropagating with the atoms (pushing beam). This setup comes close to the $2D^+$-MOT of Dieckmann et al [12]. The new longitudinal velocity distribution is shown in Fig. 10. A narrow (width $\approx$7.5 m/s) and intense peak at low velocities (centered around 25 m/s) rises. The width of this feature increases and its position is shifted towards higher values when the power in the pushing beam is increased. Since there is no magnetic field gradient on the axis, the axial beam addresses only a certain velocity class of atoms. The data indicates that a group of atoms propagating in the negative z-direction is slowed down and their direction of propagation is turned around into the positive z-direction. At the same instance the very slow atoms are pushed out of the beam. The velocity distribution shows almost no atoms at velocities below 15 m/s. The total flux stays nearly constant when shining in the pushing beam. Only for high powers (above 15 mW) in the pushing beam the

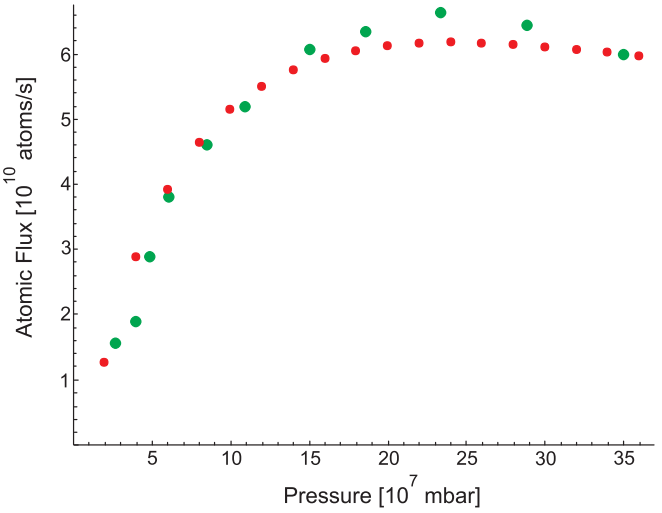

FIG. 9: Dependence of the atomic flux on the Rb-pressure in the vapor cell. The dark spots mark the theoretical results whereas the bright circles describe the experimental results. The measurement was done at full length of the MOT laser beams (92 mm) and at a laser power of 170 mW. At low pressures the atomic flux increases linearly whereas it finds a maximum at about $2{\cdot}10^{-6}$ mbar and decreases for higher values. The mean free path in the cell reaches the value of the length of the MOT at the pressure for the maximum flux - a clear hint that collisions limit a further increase of the atomic flux. The theoretical model agrees well with the experimental data.

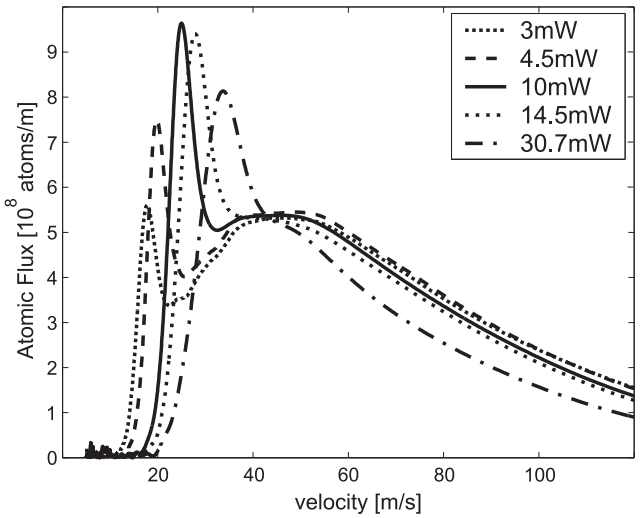

FIG. 10: When a laser beam is shone on the axis copropagating with the atomic beam, the longitudinal velocity distribution changes dramatically. A narrow peak rises up at velocities between 20 m/s and 40 m/s. Its width and position on the v_z-axis depends on the intensity in the pushing beam. Atoms at very low velocities below 15 m/s are pushed out of the beam or are accelerated. The total flux stays nearly constant.

2D-MOT is too much disturbed and the flux decreases as is shown by the curve for 30.7 mW in Fig. 10. A different detuning in the axial beams from the usual MOT-laser beams could address the high velocity classes and increase the number of slow atoms in the beam. This slowing effect can be used to increase the flux at low velocities which might be useful when loading conventional 3D-MOT configurations with capture ranges around 30 m/s.

We verified the results of the TOF technique with the method of Doppler-spectroscopy directly on the atomic beam. For that purpose another light sheet from the probe laser was aligned counterpropagating to the atomic beam at an angle of 3.5° to it. When scanning the laser-frequency one obtains Doppler-profiles which confirm the longitudinal velocity profiles of the beam obtained by the TOF-measurements. In this measurement we could verify that the thermal background transmitted by the differential pumping tube is negligible compared to the high flux of cold atoms.

IV. SUMMARY AND OUTLOOK

We have realized and investigated a novel setup for an intense source of slow atoms. The underlying physics is pure two-dimensional cooling and trapping. To reach a high flux with a small divergence we work at high vapor pressures and with a long cooling region. The length of the 2D-MOT provides good collimation (divergence $\approx$ 32 mrad) and a mean velocity of 50 m/s. The high vapor pressure assures a large loading rate and thus a high flux. To be able to work at pressures in the range of 10^{-6} mbar we work with four separate counterpropagating cooling laser beams. The total flux is in the range of several 10^{10} atoms per second. A maximum flux of $6 \cdot 10^{10}$ atoms/s was obtained at a 2D-MOT length of 90 mm, laser intensity of 160 mW per beam and a vapor pressure in the glass cell of $1.6 \cdot 10^{-6}$ mbar.

This alternative source of atoms provides a total flux comparable to a Zeeman slower with less total length, less material throughput and without disturbing light and magnetic fields for a consecutive MOT in a UHV system and therefore provides a very good starting point for further laser and evaporative cooling experiments and BEC-generating apparatus [18, 19].

In a consecutive experiment we loaded the beam into a 3D-MOT with a capture velocity of about 50 m/s which traps a large fraction of the atoms.

Acknowledgement

This work was supported by the Schwerpunktprogramm: "Wechselwirkung in ultrakalten Atom- und Molekülgasen" (SPP 1116) of the Deutsche Forschungs-

gemeinschaft and by the European Research Training Network: "Cold Quantum Gases" under the contract No: HPRN-CT-2000-00125.

[1] C.S. Adams, M. Sigel and J. Mlynek, Phys. Rep. **240**, 143 (1994).

[2] H.J. Metcalf, P. van der Straten, *Laser Cooling and Trapping*, Springer, New York (1999), ISBN 0-387-98728-2.

[3] W. Ketterle, N.J. van Druten, Evaporative Cooling of Trapped Atoms, Adv. At. Mol. Opt. Phys., **37**, 181 (1996).

[4] W. Phillips and H.J. Metcalf, PRL. **48**, 596-599 (1982).

[5] Z.T. Lu, K.L. Corwin, M.J. Renn, M.H. Anderson, E.A. Cornell, and C.E. Wieman, Phys. Rev. Lett. **77**, 3331 (1996).

[6] E. Riis, D.S. Weiss, K.A. Moler, S. Chu, Phys. Rev. Lett. **64**, 1658 (1990).

[7] T.B. Swanson, N.J. Silva, S.K. Mayer, J.J. Maki, D.H. McIntyre, JOSA B **13**, 9, 1833 (1996).

[8] H. Chen, E. Riis, Appl. Phys. B **70**, 665 (2000).

[9] J. Nellessen, J. Werner, W. Ertmer, Opt. Comm. **78**, 300 (1990).

[10] J. Yu, J. Djemaa, P. Nosbaum, P. Pillet, Opt. Comm. **112**, 136 (1994).

[11] P. Berthoud, A. Joyet, G. Dudle, N. Sagna, P. Thomann, Europhys. Lett. **41**, 141 (1998).

[12] K. Dieckmann, R.J.C. Spreeuw, M. Weidemüller and J.T.M. Walraven, Phys. Rev. A **58**, 3891 (1998).

[13] A. Camposeo, A. Piombini, F. Cervelli, F. Tantussi, F. Fuso, E. Arimondo, Opt. Comm. **200**, 231 (2001).

[14] C. Monroe, W. Swann, H. Robinson and C. Wieman, Phys. Rev. Lett. **65**, 1571 (1990).

[15] A.M. Steane, M. Chowdhury and C.J. Foot, JOSA B, **9**, 2142 (1992).

[16] E.J.D. Vredenbregt, K.A.H. van Leeuwen, H.C.W. Beijerinck, Opt. Comm. **147**, 375 (1998).

[17] M.H. Hablanian, *High-Vacuum Technology*, M. Dekker, New York (1990), ISBN 0-8247-8197-X.

[18] W. Ketterle, D.S. Durfee, and D.M. Stamper-Kurn, Proceedings of the International School of Physics "Enrico Fermi", Course CXL, IOS Press, Amsterdam, 1999) pp. 67-176.

[19] E. Mandonnet, A. Minguzzi, R. Dum, I. Carusotto, Y. Castin and J. Dalibard, Eur. Phys. J. D **10**, 9-18 (2000).